

Aero-acoustic investigation over a 3-dimensional open sunroof using CFD

Ashish Singh¹, Shrikant Sude², Nilay Chavda³, Nishita Ravuri⁴

^{1,2,3,4}Student, Department of Aerospace Engineering, MIT ADT University, Maharashtra, India

Abstract - Buffeting noise, a common phenomenon observed in moving vehicles, is an acoustic response due to the difference in aerodynamics around openings like sunroofs and side windows. The reduction of the resultant acoustic noise has been the area of interest of aerodynamicists. The research work of this project aims to establish the basis for the design of a deflector that solves the problem of sunroof buffeting noise in a three-dimensional simplified car model. This will be executed through Computational Fluid Dynamics (CFD) numerical simulation technology. The pressure characteristics of buffeting noise at different speed conditions are to be analyzed. The pressure distribution around the sunroof will help establish an efficient design for a deflector. The Detached Eddy Simulation (DES) method is chosen for this analysis because it is conventionally used for acoustic-based studies. Additionally, since the conditions at maximum noise are intended to be modelled, compressibility is incorporated in the fluid model. The domain around the car model will be constructed to replicate a three-dimensional wind tunnel, and the boundary conditions will be assigned accordingly. The observations obtained about buffeting will be used to brainstorm the design, sizing and positioning of the deflector.

Key Words: Aeroacoustics, CFD, Detached-Eddy simulations, Buffeting, Virtual Wind Tunnel, Car sunroof, Sunroof deflectors

1. INTRODUCTION

The unpleasant, low-frequency, high-sound-pressure-level noise observed around sunroofs and side windows of moving vehicles is termed as buffeting. The occurrence of this phenomenon is dependent on various factors, primary ones being vehicle speed and geometry. It happens when the air particles around the geometry collide with the surfaces and other geometries. Every vehicle has a critical speed and condition at which buffeting occurs. Generally, a sound intensity level greater than 110 dB and a frequency of less than 20 Hz characterize buffeting [1].

The specimen used for testing in this project is an extension of the Ahmed body. This simplified car model is simulated in a 3-D virtual domain. In order to replicate a wind tunnel for this domain, two sets of inlets were used, a pressure inlet and velocity inlet. The simulations are carried out for two primary cases at different velocities- closed sunroof and open sunroof. As previously stated, buffeting

occurs at a critical speed, and the aim of this project is to study and demonstrate the same.

2. LITERATURE SURVEY

1. Study on the sunroof buffeting suppression with a notched flat deflector [2]: This paper has implemented a simulation method to investigate the sunroof buffeting phenomena of the vehicle with castled deflector with velocity range of 30 km/h-90 km/h. At 70 km/h, the maximum buffeting occurred, with a magnitude of 135.9 db. A notched flat deflector was used instead of a castled deflector to decrease buffeting. The results revealed a considerable reduction in sound pressure, with buffeting noise dropping to 97.9 db.
2. The Effect of a Sheared Crosswind Flow on Car Aerodynamics [3]: The aerodynamic parameters of a DrivAer model in fastback and squareback form, subject to a crosswind flow, with and without shear, were analyzed using a CFD simulation in this work. The yaw simulation was performed with a 10° yaw angle and one shear flow exponent. It has been observed that the car experiences similar forces and moments in both the cases when the mass flow in the crosswind over the height of the car is identical.
3. Aerodynamics of High-Performance Vehicles [4]: The purpose of this research is to improve the racing vehicle's exterior fluid dynamics and to investigate the notion of various aerodynamic properties and their effects on racing automobiles. Aerodynamically, race cars are designed to reduce drag, reduce vehicle resistance, and increase downforce. Although downforce is utilized to offer stability when driving through turns, drag forces limit maximum speed and affect fuel consumption. The effect of aerodynamics on various racing car parameters and CFD has been reviewed in this work.
4. Assessing the Effects of Shear and Turbulence During the Dynamic Testing of the Crosswind Sensitivity of Road Vehicles [5]: This research focuses on the issue of crosswind sensitivity at greater speeds as well as weight reduction in modern cars. The fluctuation in vertical velocity profile as well as the turbulence severity within the gust were considered using a generic squareback model. Because there was less variance in turbulence

intensity and the vertical velocity profile was varied, the results showed a significant difference in aerodynamic stress on the model.

5. Wind tunnel tests and aerodynamic numerical simulations of car opening windows [6]: The article focuses on the aerodynamic drag caused by varying window opening levels in both the wind tunnel and aerodynamic numerical simulation. The results of both approaches were analyzed, and suggestions for driving a car at a moderate pace in the summer were offered. It was discovered that when the car's air conditioner is turned on, it consumes more gasoline than when the car's windows are open at a speed less than 90 km/h.
6. Computational study of flow around a simplified car body [7]: The flow around the Ahmed body was explored numerically for the base slat angles of 25 and 35 degrees in this research. The transition of the wake to completely three-dimensional behavior is not recreated for slant angle 25°, although the two-dimensional behavior of the flow is accurately anticipated for slant angle 35°.
7. Computational aero-acoustic analysis of a passenger car with a rear spoiler [8]: This research proposed a numerical model based on a CFD technique to estimate the flow structure around a passenger automobile with a wing-type rear spoiler. The CFD solver used in this investigation is Ansys Fluent (19.2). The aerodynamic lift coefficient can be reduced by installing a spoiler with an adequate angle of attack. Additionally, installing an endplate might help to decrease noise from behind the vehicle. It is obvious that a passenger vehicle's vertical stability and noise reduction may be enhanced. Eventually, the most appropriate spoiler design's aerodynamics and aeroacoustics are introduced and examined.
8. Experimental and numerical study of the flow field around a small car [9]: The main objective of this work is to comprehend the flow field and do an aerodynamic analysis on a small car. CFD Fluent is used to do the numerical simulation in order to determine the vehicle's drag force as well as the flow field. Particle image velocimetry (PIV) is then used to investigate the flow field surrounding the vehicle in a wind tunnel. When the computational and experimental flow fields are compared, they reveal an excellent match.
9. Experimental and computational study of vehicle surface contamination on a generic bluff body [10]: The goal of this work is to give an experimental and numerical (CFD) investigation of methodologies used to describe vehicle surface pollution caused by rear wake aerodynamics. The contamination is investigated in a wind tunnel under controlled conditions using a typical bluff body (the Windsor model.) CFD results were

obtained utilizing particle tracking techniques and both stable RANS and unsteady URANS solvers. Steady RANS does not correctly capture the wake structures, which has an impact on contamination prediction. The large-scale wake unsteadiness found in the experimental data is recovered by URANS, but the discrepancy between the experimental and computational contamination distributions remains essential.

10. Computational study of the unsteady flow structures around two vehicles [11]: This research exhibits the evolution of two vehicle models as well as the impact of various unstable aerodynamic circumstances on the vehicle's handling. When a car moves at high speeds, the pressure imposed on the back-end changes unexpectedly, whilst the pressure surrounding the front remains relatively constant pressure, temperature, Mach number, and velocity. The flow around the minivan exhibits quasi-periodic vortex shedding, resulting in a significant increase in surface pressure. In the instance of the pick-up truck, the surface pressure reveals an arch-like shape. Irjet Template sample paragraph. Define abbreviations and acronyms the first time they are used in the text, even after they have been defined in the abstract. Abbreviations such as IEEE, SI, MKS, CGS, sc, dc, and rms do not have to be defined. Do not use abbreviations in the title or heads unless they are unavoidable.

3. METHODOLOGY

This section explains the process that was adopted to carry out the simulations. After creating the geometry of the specimen and the domain, the entire model was meshed on the Ansys Workbench. This meshed file was then imported on Ansys Fluent for the analysis. The following sections explain the procedure in detail

3.1 Solver Setup

For the prediction of velocity at different locations in the X-direction, several points are created, at which the flow is to be monitored (also called probe points). The same is shown in Fig 3.

An unsteady simulation is run for two values of input velocities, namely at 60 km/h and 100 km/h wind speed. The car model considered without sunroof (also referred to as the closed case) represents non-buffeting simulation, while the case where the sunroof is open (also referred to as open sunroof case) represents buffeting simulation.

It may be noted that the boundary conditions for both the cases are the same and have been tabulated (Table 2). A scale resolving detached eddy simulation is selected. Further implementation of the Detached Eddy simulation Spallart-Allmaras (DES-SA) model on Ansys Fluent 19.2 has been implemented.

Table-1: Solver setup

Function	Setting
Solver	Pressure-based, unsteady, least square cell based
Fluid material	Air as ideal gas
Time formulation	Second-order implicit
Turbulence model	DES-SA (SA production vorticity based)
Pressure-velocity coupling	SIMPLEC
Pressure discretization	Second-order
Momentum discretization	Bounded central differencing
Modified turbulence viscosity	Second-order upwind
Energy discretization	Second-order upwind

With the solver setup settings from Table 1, the simulations were run for 60 km/h and 100 km/h on a closed and an open sunroof case

Boundary label	Boundary condition	Value
Nozzle inlet	Velocity inlet (magnitude, normal to boundary)	U = 60 km/h, 100 km/h
Tunnel inlet	Pressure inlet	Gauge pressure = 0 Pa
Tunnel outlet	Pressure outlet	Gauge pressure = 0 Pa
Tunnel top, floor sides	Euler's wall (No-slip condition)	NA

In ANSYS Fluent, operating pressure is kept at 101325 Pa. To study the phenomena of buffeting for such cavity using computational fluid dynamics can be more efficient by adding compressibility in the fluid modelling. Compressibility precisely propagates the pressure waves at

the local speed of sound in the flow field. This ensures accurate interaction between solid body and fluid. This interaction determines buffeting frequency and propagation of resultant pressure waves inside the cavity volume.

3.2 Solution procedure for simulation

Each speed case for buffeting simulation is first run-in steady state mode for 14400 iterations and then unsteady state. Unsteady state simulation provides time dependent results. A time step of 0.005 is calculated to run the flow as desired frequency range is 0-50 Hz. Within each time step 12 number of maximum iterations are allowed. The total number of time steps were 1200. The three pressure probes are located inside the car volume viz. (-0.36, 0, 1), (-0.56, 0, 1) and (-0.76, 0, 1).

These vertices are defined to be vertex average with static pressure as a recording parameter. The pressure fluctuation meets gradual stability with increase in time. After 1200-time steps, 100 samples are noted on above mentioned 3 vertices. To enable aero-acoustic analysis, Fast Fourier Transformation (FFT) with Hanning window is utilized. Sound pressure level is defined as:

$$SPL = 20 \log \left(\frac{P}{P_0} \right)$$

where P is the sound pressure of the noise in Pa, and P₀ is the reference pressure equal to 2 x 10⁻⁵ Pa.

3.3 Simplified car model analysis without sunroof

1. Geometry Information:

The geometric dimensions of the simplified car model without sunroof are used for experimental investigation of buffeting noise as shown in Fig 1.

For our study, we have constructed a virtual wind tunnel with suitable size as given in Fig.2. To carry out volume discretization as well as surface discretization, ANSYS 19.2 is engaged

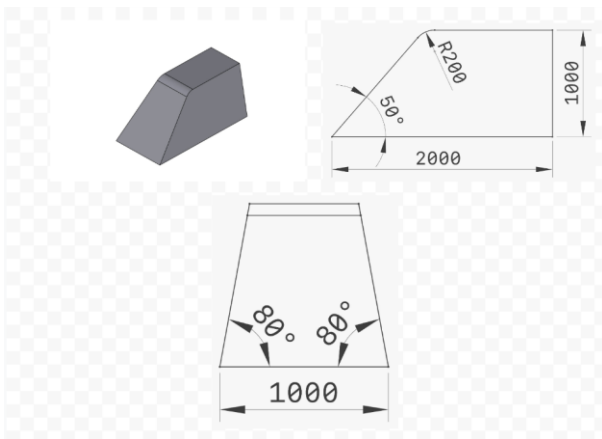


Fig-1: (clockwise) Isometric, side, and front views of specimen for case without sunroof

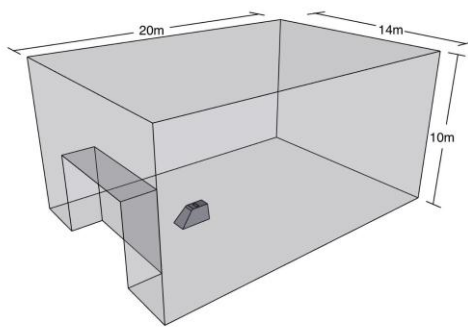


Fig-2: Geometry of chosen domain

2. Mesh Information

The simplified car model is placed in virtual wind tunnel as given in Fig3. In this discretization process, hexacore, tetrahedral and prism elements were selected. A layered mesh consisting of 20 prism layers is generated to capture boundary layer phenomena precisely. The first cell height of 0.00025 m and a uniform growth ratio of 1.15 are inserted. While doing discretization, researchers have kept in their mind that the grid near the model is fine and away from the model is coarse. To achieve this desired form of mesh, three spheres of influence are used. The domain is said to be fluid zoned, and the simplified car model is said to be solid.

The total mesh count is approximately 8 million cells. For accurate prediction of velocity and pressure near the boundary walls of model, prism layers are used.

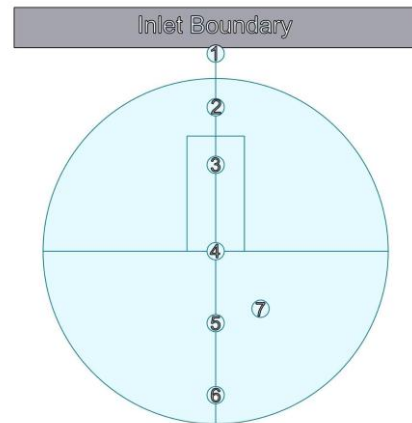


Fig-3: Points at which the flow is intended to be monitored

3.4 Simplified car model analysis with sunroof

1. Geometry Information:

The geometric dimensions of the simplified car model with sunroof are used for experimental investigation of buffeting noise as shown in Fig 1.

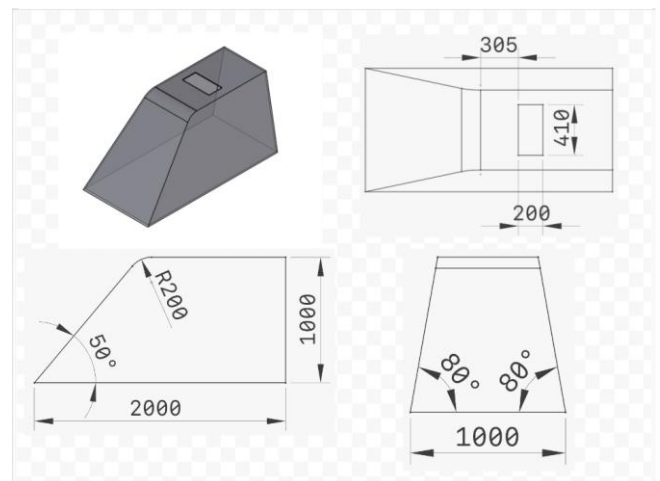


Fig-4: (clockwise) Isometric, top, front and side views of the specimen for open sunroof case

In Fig 4, to investigate the buffeting phenomenon an open sunroof of dimension (410mm x 200mm) is created. The thickness of the car model is 10 mm.

2. Mesh Information

The entire discretization process of without sunroof car model is precisely followed for this case. Although, a volume mesh is generated inside the model to create a probe point inside the model and to allow the fluid to enter the cavity. The total mesh count for this case is 10 million cells.

4. SIMULATION RESULTS

A. To analyze the flow over the model, a cut plane aligned with the plane and $y = 0$ is displayed.

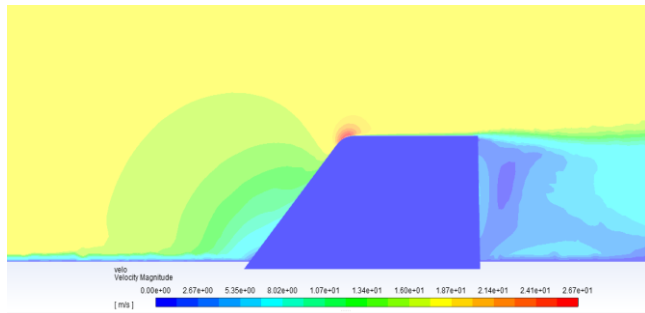


Fig-5: Velocity contour around specimen for closed-sunroof case at 60km/h velocity

The velocity magnitudes in closed car model are analyzed quantitatively using several probe points mentioned in Fig 3. This case is simulated as a precursor to the primary case of interest, i.e., when the sunroof is open. The buffeting noise inside the closed-car model is not in the scope of this paper. The buffeting simulation is carried out at 60 km/h and 100 km/h. The results of the simulation for closed case at a velocity of 60 km/h is presented in Fig. 5.

Upon establishing a visual and quantitative representation of the velocity flow around the selected geometry, the case for the open sunroof was simulated. The velocity profiles of the simulation are presented in Fig. 6 and 7. To understand the oscillatory behavior of the open case, the frequency spectra at both the aforementioned speeds are plotted, which may be seen in Fig.8.

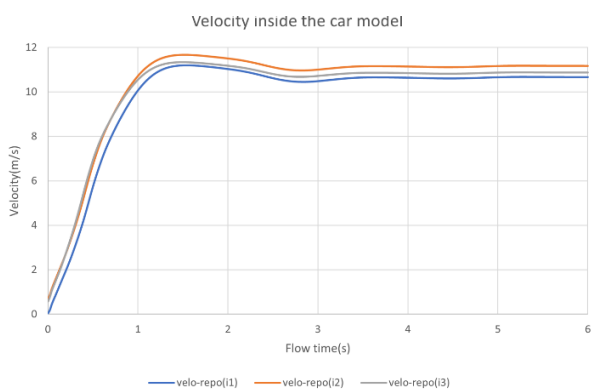


Fig-6: Velocity profile for open sunroof case at 60 km/h

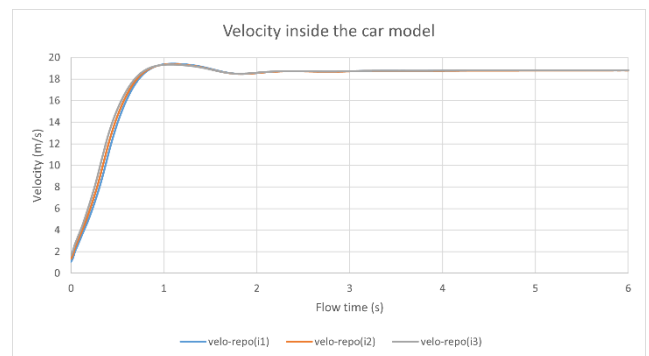


Fig-7: Velocity profile for open sunroof case at 100 km/h

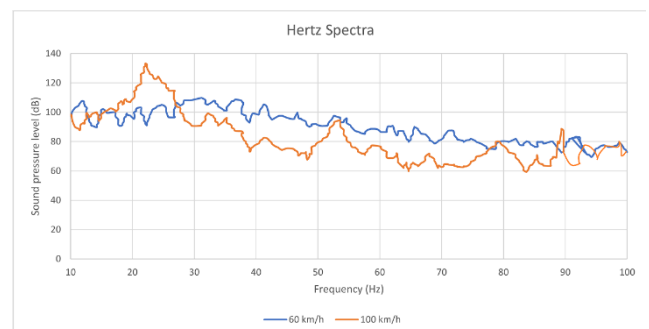


Fig-8: FFT plot of open sunroof case at velocities 60 km/h and 100 km/h

It is evident from the graph in Fig. 8, that high buffeting noise is captured with 60 km/h velocity. The reason behind low buffeting at 100 km/h is due to most of the flow rushes over the cavity with weak stream coming inside the car model.

5. CONCLUSIONS AND FUTURE WORK

The dependency of buffeting on the velocity of the vehicle has been demonstrated and it may be inferred that each vehicle has a critical speed at which buffeting is most likely to occur. As previously mentioned, the geometry of the vehicle also plays an important role in determining the occurrence of buffeting.

The existing paper gives rise to the study of modelling a sunroof deflector that can efficiently overcome buffeting. The same methodology followed in this paper may be followed to understand the flow around the new specimen, that consists of a deflector. The size, location, orientation and shape of the deflector may be determined by creating and checking various cases.

ACKNOWLEDGEMENT

This paper would not have been possible without our project mentor Prof. Dr. Devabrata Sahoo. We are grateful for his support, guidance, and encouragement through the course of the project.

We also sincerely thank the Head of Department, Aerospace Engineering at MIT School of Engineering, MIT-ADT University, Pune.

REFERENCES

- [1] Zhang, Q.; He, Y.; Wang, Y.; Xu, Z.; Zhang, Z. (2020) 'Computational study on the passive control of sunroof buffeting using a sub-cavity.' *Appl. Acoust*, 159, 1–9
- [2] Y. *et al.* (2019) 'Study on the sunroof buffeting suppression with a notched flat deflector', *INTER-NOISE 2019 MADRID - 48th International Congress and Exhibition on Noise Control Engineering*.
- [3] Howell, J., Forbes, D., Passmore, M., & Page, G. (2017). 'The Effect of a Sheared Crosswind Flow on Car Aerodynamics.' *SAE International Journal of Passenger Cars - Mechanical Systems*, 10(1), 278–285. <https://doi.org/10.4271/2017-01-1536>
- [4] Kshirsagar, V. and Chopade, J. V. (2018) 'Aerodynamics of High-Performance Vehicles', *International Research Journal of Engineering and Technology*, 5(3), pp. 2182–2186. Available at: <https://www.irjet.net/archives/V5/i3/IRJET-V5I3502.pdf>.
- [5] MacKlin, R., Garry, K. and Howell, J. (1997) 'Assessing the effects of shear and turbulence during the dynamic testing of the crosswind sensitivity of road vehicles', *SAE Technical Papers*, (412), pp. 27–40. doi: 10.4271/970135
- [6] Zhang, Y. C., Zhao, J., Li, J., & Zhang, Z. (2012). 'Wind tunnel tests and aerodynamic numerical simulations of car opening windows.' *International Journal of Vehicle Design*, 62. <https://doi.org/10.1504/ijvd.2012.045923>
- [7] Guilmineau, E. (2008). 'Computational study of flow around a simplified car body.' *Journal of Wind Engineering and Industrial Aerodynamics*, 96(6–7), 1207–1217. <https://doi.org/10.1016/j.jweia.2007.06.041>
- [8] Tsai, C. H., Fu, L. M., Tai, C. H., Huang, Y. L., & Leong, J. C. (2009). 'Computational aero-acoustic analysis of a passenger car with a rear spoiler.' *Applied Mathematical Modelling*, 33(9), 3661–3673. <https://doi.org/10.1016/j.apm.2008.12.004>
- [9] Dobrev, I. *et al.* (2017) 'Experimental and numerical study of the flow field around a small car', *MATEC Web of Conferences*, 133, pp. 0–3. doi: 10.1051/mateconf/201713302004.
- [10] Kabanovs, A. *et al.* (2016) 'Experimental and Computational Study of Vehicle Surface Contamination on a Generic Bluff Body', *SAE Technical Papers*, (April). doi: 10.4271/2016-01-1604.
- [11] Tutunea, D., Bica, M. and Dima, A. (2014) 'Computational Study of the Unsteady Flow Structures Around Two Vehicles', *Journal of Industrial Design and Engineering Graphics*, 9(1), pp. 13–16.